Phycologia (2013) Volume 52 (3), 266–278 Published 3 May 2013

Phylogeny of the genus *Mallomonas* (Synurophyceae) and descriptions of five new species on the basis of morphological evidence

Bok Yeon Jo[1], Woongghi Shin[1*], Han Soon Kim[2], Peter A. Siver[3] and Robert A. Andersen[4]

[1]*Department of Biology, Chungnam National University, Daejeon 305–764, Korea*
[2]*Department of Biology, Kyungpook National University, Daegu 702-701, Korea*
[3]*Department of Botany, Connecticut College, New London, Connecticut 06320, USA*
[4]*Friday Harbor Laboratories, University of Washington, Friday Harbor, Washington 98250, USA*

Jo B.Y., Shin W., Kim H.S., Siver P.A. and Andersen R.A. 2013. Phylogeny of the genus *Mallomonas* (Synurophyceae) and descriptions five new species on the basis of morphological evidence. *Phycologia* 52:266–278. DOI: 10.2216/12–107.1

We used a molecular analysis based upon three genes, coupled with the ultrastructure of scales and bristles, to investigate phylogenetic relationships within *Mallomonas*, with a focus on the section *Planae*. Fossil taxa discovered in Middle Eocene lacustrine deposits from northwestern Canada were used to calibrate a relaxed molecular clock analysis and investigate temporal aspects of species diversification. Four new extant species, *Mallomonas lacuna, M. hexareticulata, M. pseudomatvienkoae*, *M. sorohexareticulata,* and one new fossil species, *M. pleuriforamen*, were described on the basis of morphological differences, including the number, distribution, and size of base plate pores, the secondary structures on scale surfaces, and characteristics of the bristles. Four of the new species align with *M. matvienkoae* and the fifth with *M. caudata*. Molecular phylogenetic analyses inferred using nuclear-encoded small-subunit ribosomal (r)DNA and large-subunit rDNA and plastid-encoded *rbc*L sequences placed four of the new species with *M. matvienkoae*, the fifth with *M. caudata*, all in a strongly supported clade within the section *Planae*. A Bayesian relaxed clock analysis showed that the genus *Mallomonas* diverged into two major clades about 133 Ma (Early Cretaceous), one of which represents the section *Planae*. The earliest diverging lineage within the section *Planae* was *M. bangladeshica*, followed by *M. heterospina* and *M. oviformis*, and most recently by *M. sorohexareticulata* and *M. hexareticulata*.

Key Words: Cretaceous, *Mallomonas*, Molecular phylogeny, Morphology, Scale, Ultrastructure

INTRODUCTION

Criteria for the classification and delineation of infrageneric ranks and species within the genus *Mallomonas* are based largely on cell morphology and characteristics of the siliceous components covering the cell (Krieger 1930; Conrad 1933; Matvienko 1941; Harris & Bradley 1960; Momeu & Péterfi 1979; Asmund & Kristiansen 1986; Siver 1991; Kristiansen 2002; Kristiansen & Preisig 2007). Matvienko (1941) erected the genus *Mallomonopsis* to accommodate species with two, not one, emergent flagella, which included *Mallomonas matvienkoae* (Matvienko) Asmund & Kristiansen. Belcher (1969) rejected this separation and suggested that species with two emergent flagella be placed in a subgenus within *Mallomonas*. Following Belcher's suggestion, Momeu and Péterfi (1979) created two subgenera (*Mallomonas* and *Mallomonopsis*) and seven sections. In the more recent classification systems of Asmund and Kristiansen (1986) and Siver (1991), the subgenus *Mallomonopsis* was treated at the section level rather than as a subgenus. Thus, the section *Mallomonopsis* coexisted with the section *Planae*. Finally, Kristiansen (2002) combined both sections *Planae* and *Mallomonopsis* to the section *Planae* because of its taxonomic priority, and placed all species with scales lacking a dome and V-rib into the section *Planae*. In this system, the section *Planae* was further divided into four series: *Caudata*, *Matvienkoae*, *Teilingianae*, and *Peronoides*.

Recent molecular work showed that the genus *Mallomonas* was divided into two major clades that were morphologically differentiated by the presence/absence of a V-rib on the siliceous scales (Jo *et al.* 2011). Since the clade lacking scales with a V-rib included section *Planae* and section *Heterospinae*, the authors suggested that species in the section *Heterospinae* be transferred to the section *Planae*. In addition, *Mallomonas* series *Matvienkoae* was not monophyletic. The main objectives of our study were (1) to understand the phylogenetic relationships within *Mallomonas* section *Planae*; (2) to describe five new species; and (3) to infer divergence times of the *Mallomonas* species on the basis of fossil and molecular data.

MATERIAL AND METHODS

Strain information and accession numbers are listed in Table S1. The 30 strains of *Mallomonas* were collected from small ditches, ponds, and swamps in Korea, and eight strains were obtained from the Provasoli-Guillard National Center for Culture of Marine Algae and Microbiota (NCMA, East Boothbay, Maine, USA), http://ncma.bigelow.org/). Culture methods followed those previously described (Jo *et al.* 2011). For field-emission scanning electron microscopy (SEM), cells were filtered using nylon membrane filters (Whatman Ltd., Maidstone, UK), rinsed in distilled water, fixed in 1% OsO_4,

* Corresponding author (shinw@cnu.ac.kr).

dehydrated, prepared, and viewed according to Jo *et al*. (2011). Voucher specimens were stored at the Chungnam National University (CNUK) herbarium in Daejeon, Korea.

Fossil scales of *Mallomonas* were collected from the Middle Eocene lacustrine facies from the Giraffe kimberlite fossil locality (64°48′N, 110°04′W) in northwestern Canada. Mudstone chips from the Giraffe core were oxidized using 30% H_2O_2 under low heat for a minimum of an hour, forming a slurry. After washing with distilled water, an aliquot of each sample was air dried onto heavy-duty aluminium foil. The aluminium foil samples were trimmed, attached to aluminium stubs with Apiezon® wax (Apiezon, Manchester, UK), coated with a mixture of gold and palladium for 2 min with a Polaron Model E sputter coater (Ladd Research, Williston, Vermont, USA), and examined with a Leo 982 field-emission SEM (Zeiss/LEO, Oberkochen, Germany).

DNA extraction, polymerase chain reaction amplification procedure, purification, sequencing, and sequence alignment were conducted as described by Jo *et al*. (2011). The sequences for the nuclear-encoded small-subunit (SSU) ribosomal (r)DNA and large-subunit (LSU) rDNA were aligned by eye using as a guide the secondary structure of the rDNA gene sequences of *M. annulata* (Bradley) Harris (Wuyts *et al*. 2001). The conserved areas of the two genes were readily aligned across taxa and were used for phylogenetic analyses. Therefore, unalignable nucleotides were excluded in phylogenetic analyses as well as pair-wise comparisons. The alignment of *rbc*L gene sequences was based on the alignment of the inferred amino acid sequence; the first and second codons were used for phylogenetic analyses, but the third codon was deleted because of multiple hits. The sequence similarities were calculated using pair-wise distances [(1 − each pair-wise distance value) × 100] using the PAUP*, Version 4.0b10 (Swofford 2002) on the basis of a combined data set of aligned unambiguous sequences for phylogenetic analyses.

A combined data set of 4958 characters (SSU rDNA = 1667, LSU rDNA = 2576, and *rbc*L = 715) was generated for phylogenetic analysis. The sequences of four outgroup chrysophycean species were used to root the tree. The maximum likelihood (ML) phylogenetic analyses were done using the RAxML 7.0.4 program (Stamatakis 2006) with the general time reversible (GTR) model. We used 1000 independent tree inferences using -# option of the program to identify the best tree. Bootstrap values were calculated using 1000 replicates using the same substitution model. Bayesian analyses were run using MrBayes 3.1.2 (Huelsenbeck & Ronquist 2001) with a random starting tree and run for 2×10^6 generations, keeping on tree every 1000 generations. Each analysis was performed using the four Metropolis-coupled Markov chain Monte Carlo, with 2×10^6 generations for each chain. Burn-in point was identified graphically by tracking the likelihoods (Tracer V.1.5; http://tree.bio.ed.ac.uk/software/tracer/). The first 100 generations were discarded, and the remaining 1901 trees were used to calculate the posterior probabilities (PP) of each clade. Maximum parsimony (MP) and neighbor-joining (NJ) analyses were constructed on combined data set with PAUP* using a heuristic search algorithm with the following settings: 100 random sequence-addition replicates, tree bisection–reconnection branch swapping, MulTrees, all characters unordered and unweighted, and branches with a maximum length of zero collapsed to yield polytomies. The bootstrap values (BS) for the resulting nodes were assessed using bootstrapping with 1000 on both trees. For distance analyses, the program Modeltest version 3.7 (Posada & Crandall 1998) was used to determine parameters. The best-fit model for the combined data set was a $\mathrm{TrN}+\mathrm{I}+\Gamma$ model with the following parameters:BaseFreq = 0.2910, 0.1890, 0.2546, 0.2654, RateMatrix = 1.0000, 2.7270, 1.0000, 1.0000, 5.1380, 1.0000, Invariant = 0.6710, Gamma shape = 0.6245.

We used a Bayesian inference method with a relaxed clock model using BEAST ver. 1.6.2 (Drummond & Rambaut 2007) to estimate branch divergence times using the same three-gene data set. The uncorrelated lognormal model (UCLN) was used to estimate rate variation across all branches. Age estimates for fossil calibrations were treated as probabilistic priors and not point estimates (Drummond *et al*. 2006; Ho & Phillips 2009). We used lognormal priors for the split between *M. asmundiae* (Wujek & Van der Veer) Nicholls and *M. striata* Asmund, and for the split between *M. matvienkoae* Asmund & Kristiansen and *M. caudata* Ivanov. In both cases, we used an offset of 40 Ma, a mean of 0.5, and a standard deviation of 1.0. Numerous scales of *M. asmundiae* are well represented in the laminated sediments of the Giraffe Pipe core (Siver *et al*. 2009), estimated to have a minimum age of approximately 40 Ma (Siver & Wolfe 2009). In addition, we assumed that the new fossil species was closely related to modern *M. matvienkoae*. We ran analyses calibrating only the *M. asmundiae* and *M. striata* node, only the *M. matvienkoae* and *M. caudata* node, and both nodes. Age estimates were similar for all three cases, but calibrating both nodes yielded lower error estimates. We presented only the analysis calibrating both nodes. A GTR + gamma site model was applied to the three-gene concatenated data set, and a uniform Yule tree prior was used to model speciation. The analysis was run for 10 million generations with the chain sampled every 1000 generations. Convergence of parameter estimates and estimation of burn-in was checked using Tracer V. 1.5. The initial 2500 trees (2.5 million generations) were removed as burn-in and the remaining 7500 trees used to construct the final chronogram. The consensus tree, along with both 95% PP and age estimates for all branches, was visualized using Fig Tree ver. 1.3.

RESULTS

All species were identified on the basis of SEM ultrastructural features of the scale and bristle (Table 1). In addition, we described five new species, *M. lacuna, M. hexareticulata, M. pseudomatvienkoae*, *M. sorohexareticulata,* and a fossil species, *M. pleuriforamen*, on the basis of morphology of the siliceous components (Figs 1–24). The scales of the new species, which belong to the subgeneric section *Planae*, were flat, oval to elliptical in outline, possessed a proximal rim encircling about one-half of the scale perimeter, and were often slightly asymmetrical (Figs 1–24). The scales also lacked a dome, V-rib, submarginal rib, and a special area for fastening the bristle, but had base plates with evenly and

Table 1. Summary of the major diagnostic features of scales and bristles as seen with SEM and used in this study to distinguish between several closely related taxa with section *Planae* scales.

	Cell size (μm)		Obverse of scales				Reverse of scales		Bristle
Taxon	Length	Width	Dome	V-ribs	Anterior submarginal ribs	Secondary structure on the shield	Pores pattern	Specialized posterior pores	Distal part
M. bangladeshica, Hoesan061007G[1]	15.75–18.98	9.39–11.48	-	-	-	+, papillae, with internal struts	even distribution	-	needle-shaped apex
M. bronchartiana, Mulyeongari101110J[1]	50.16–54. 08	13.09–17.48	-	+	-	+, papillae, with internal reticulum	-	-	quadrifid apex
M. caudata, Dangje060207A[1]	37.05–66.67	19.38–28.00	-	-	-	-	even distribution	+, one large pore in cluster of small pores	serration
M. heterospina, Posan012608A[1]	15.56–16.25	10.25–12.50	±-	-	-	+, reticulum	even distribution except dome area	-	needle–shaped or hooked apex
M. hexareticulata, Mudong072410D[1]	12.20–18.48	7.48–11.52	-	-	-	+, secondary meshwork, each mesh roughly hexagonal	even distribution only proximal rim area	+, one large pore in cluster of small pores	divided into several-part apex
M. lacuna, CCMP2880[1]	36.07–-67.37	15.68–20.02	-	-	-	-	even distribution	+, one large pit	serration
M. matvienkoae, Mureng112807B[1]	14.25–18.41	8.25–16.22	-	-	-	+, secondary meshwork	even distribution	+, one large pore in cluster of small pores	expanded apex
M. matvienkoae var. *grandis*[2]	40–60	unknown	-	-	-	+, secondary meshwork	even distribution, become large pores toward the proximal rim area	+, three to five large proximal pores in a patch of small pores	bifurcate or expanded apex
M. matvienkoae f. *litteata*[3]	11–25	8–10	-	-	with a narrow distal submarginal rib	+, secondary meshwork	even distribution	+, one large pore in cluster of small pores	bifurcate or expanded apex
M. matvienkoae var. *myakkana*[4]	14–56	8–20	-	-	-	+, papillae	even distribution only proximal rim area	+, cluster of three to five large pores	bifurcate or expanded apex
M. matvienkoae var. *siveri*[5]	38–55	13–20	-	-	-	+, secondary meshwork	even distribution, become large pores toward the proximal rim area	+, proximal part of the scale with 12–15 larger pores	bifurcate or expanded apex
M. oviformis, Wolpo112807H[1]	18.55–22.00	16.60–21.25	-	-	-	+, papillae	even distribution	-	trifurcate apex
M. peronoides, Pihyangjeong092609A[1]	12.34–24.83	8.22–12.56	-	-	-	+, papillae, with internal struts	even distribution	-	needle-shaped apex
M.pseudomatvienkoae, Gungnam2052507A[1]	18.03–22.24	8.41–13.24	-	-	-	+, secondary meshwork	even distribution in anterior area	+, one large pore	bifurcate apex
M. sorohexareticulata, Gungnam092709[1]	28.25–35.58	7.22–15.43	-	-	-	+, papillae	even distribution except specialized posterior pore area and distal parts	+, one large pore	expanded apex

[1] This study.
[2] Dürrschmidt and Cronberg 1989.
[3] Asmund and Kristiansen 1986.
[4] Siver 1991a.
[5] Wujek and Saha 1996.

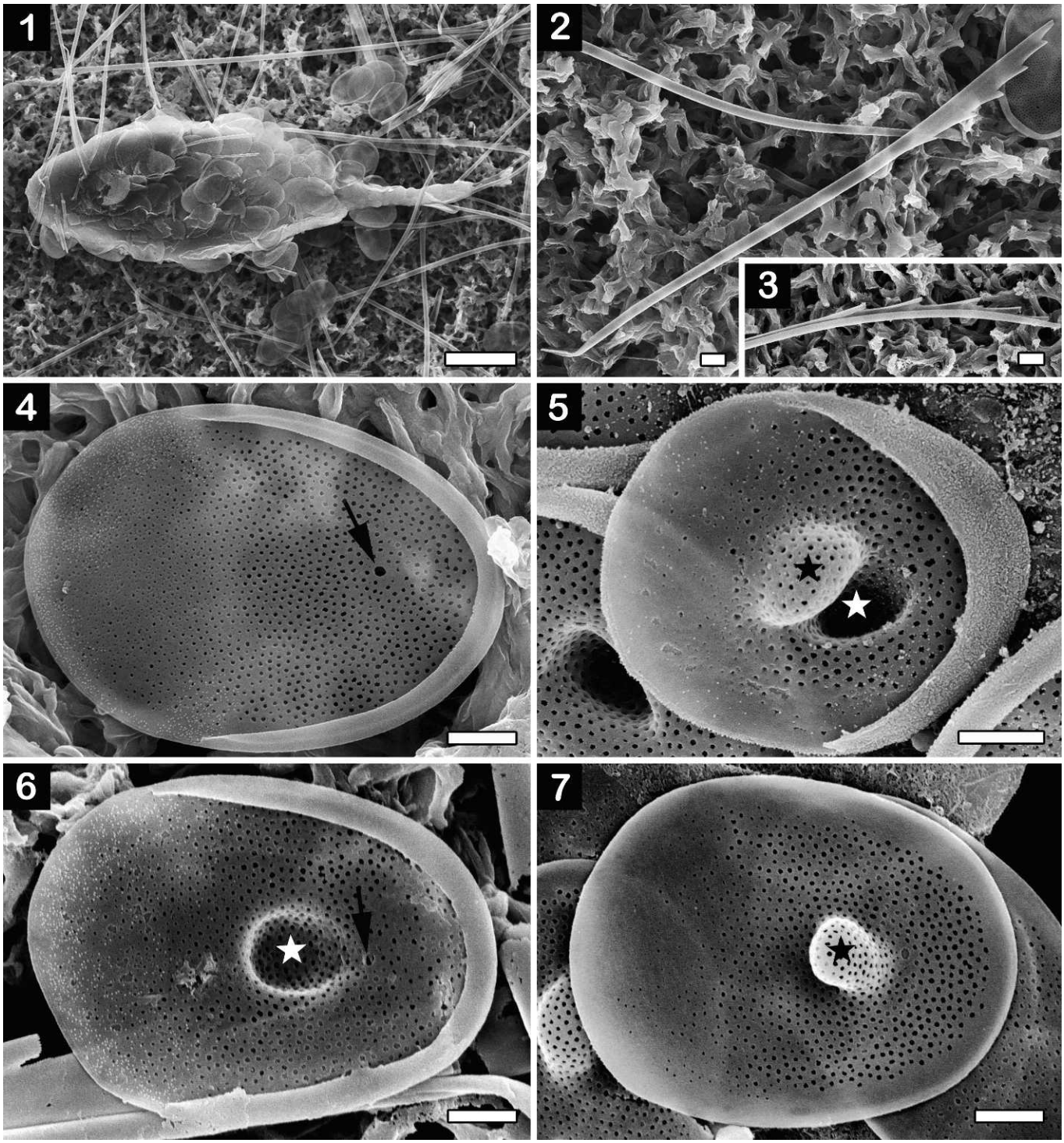

Figs 1–7. SEM micrographs of *Mallomonas lacuna* CCMP2880. For cells or scales, left sides on the figures are anterior, right sides are posterior.

Fig. 1. Ellipsoid-shaped cell with an extended caudal tail. Scale bar = 10 μm.

Fig. 2. Bristle showing the smooth side of the shaft and serrated distal end. Scale bar = 1 μm.

Fig. 3. Small inset shows the reverse side of the bristle shaft. Scale bar = 1 μm.

Fig. 4. Top surface of the scale depicting the distribution of small base-plate pores, the large single pore (arrow) in the posterior region common on all scales. Scale bar = 1 μm.

Fig. 5. Top surface of the scale depicting the distribution of small base-plate pores, the large single pore in the posterior region common on all scales and the large basket-like depression (stars) found on some specimens. Scale bar = 1 μm.

Fig. 6. Large depression (star) is situated on the anterior side of the large base-plate pore. Scale bar = 1 μm.

Fig. 7. Bottom surface of the scale showing the distribution of pores and the large protruding depression (star). Scale bar = 1 μm.

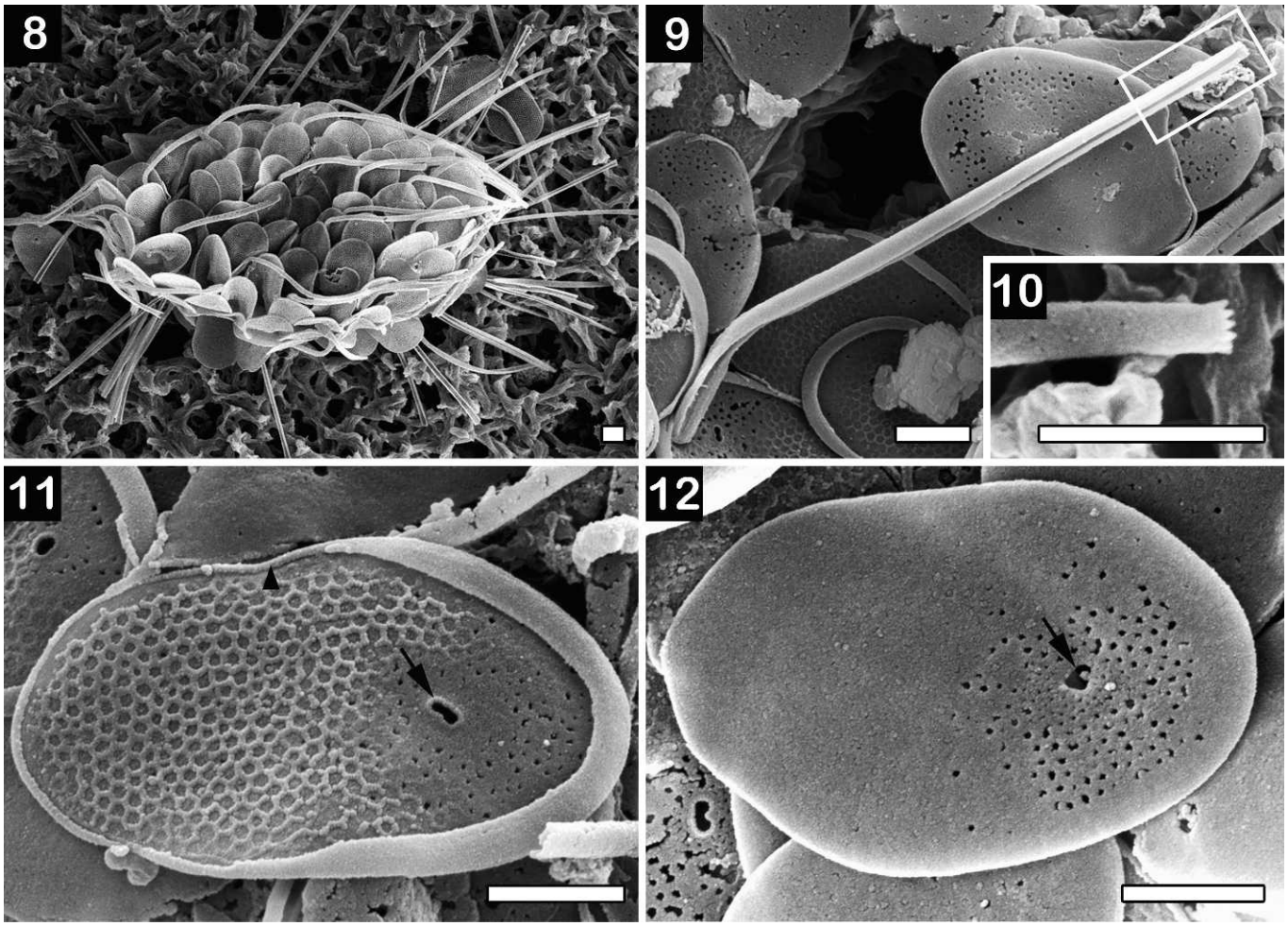

Figs 8–12. SEM micrographs of *Mallomonas hexareticulata* Mudong072410D. For cells or scales, left sides on the figures are anterior, right sides are posterior. Scale bars = 1 μm.

Fig. 8. Ovoid-shaped cell.

Fig. 9. Bristle showing an expanded proximal foot, the slit along the shaft, and the distal tip with teeth.

Fig. 10. Small inset shows the end of the bristle.

Fig. 11. Top surface of the scale depicting the expanded secondary reticulation, the unevenly shaped pores in the posterior region, the single large and elongated pore (arrow), and the posterior rim. The anterior margin of the scale is continuous with the posterior upturned rim (arrowhead).

Fig. 12. Bottom surface of the scale denoting the restriction of base-plate pores to the proximal region.

closely spaced subcircular pores. The anterior margins of the scales were lined with a rounded siliceous ridge that becomes fused to and continuous with the posterior upturned rim (arrowheads on Figs 11, 15, 19, and 24). In the middle of the proximal half of the scale one (arrows on Figs 4, 6, 12, 16, and 20) or several (arrow on Fig. 22) large pores were present, and in some species these large pores were encircled by densely spaced minute pores (Figs 12 and 23). The scales of most species were further ornamented with secondary structures, such as a surface reticulation (Figs 11 and 15) and small papillae (Figs 19 and 21).

Mallomonas lacuna Jo, Shin, Kim, Siver & Andersen *sp. nov.*

Figs 1–7

DESCRIPTION: Cells ellipsoidal (36–68 × 15–21 μm). Scales oval or obovoid, 4–7 × 3–5 μm in size; a posterior rim encircled half to two-thirds of the scale perimeter; some scale shields marked with one or two large depressions or pits; base-plate pores covering scale except along the anterior peripheral margin; posterior scale region with a large rimmed pore at the center. Bristles 11–52 μm long, smooth and slightly curved; bristle shaft tubular with a longitudinal slit and flared distal end bearing four to seven teeth along one edge.

HOLOTYPE: Collection of specimens on SEM stub deposited at the Herbarium of CNUK, Daejeon, Korea, CNU029284.

ISOTYPE: Collection of specimens on SEM stub deposited at the Herbarium of CNUK, Daejeon, Korea, CNU029699.

TYPE LOCALITY: Prebersee, Austria (47°18′60″N, 13°85′75″E), 11 July 2006.

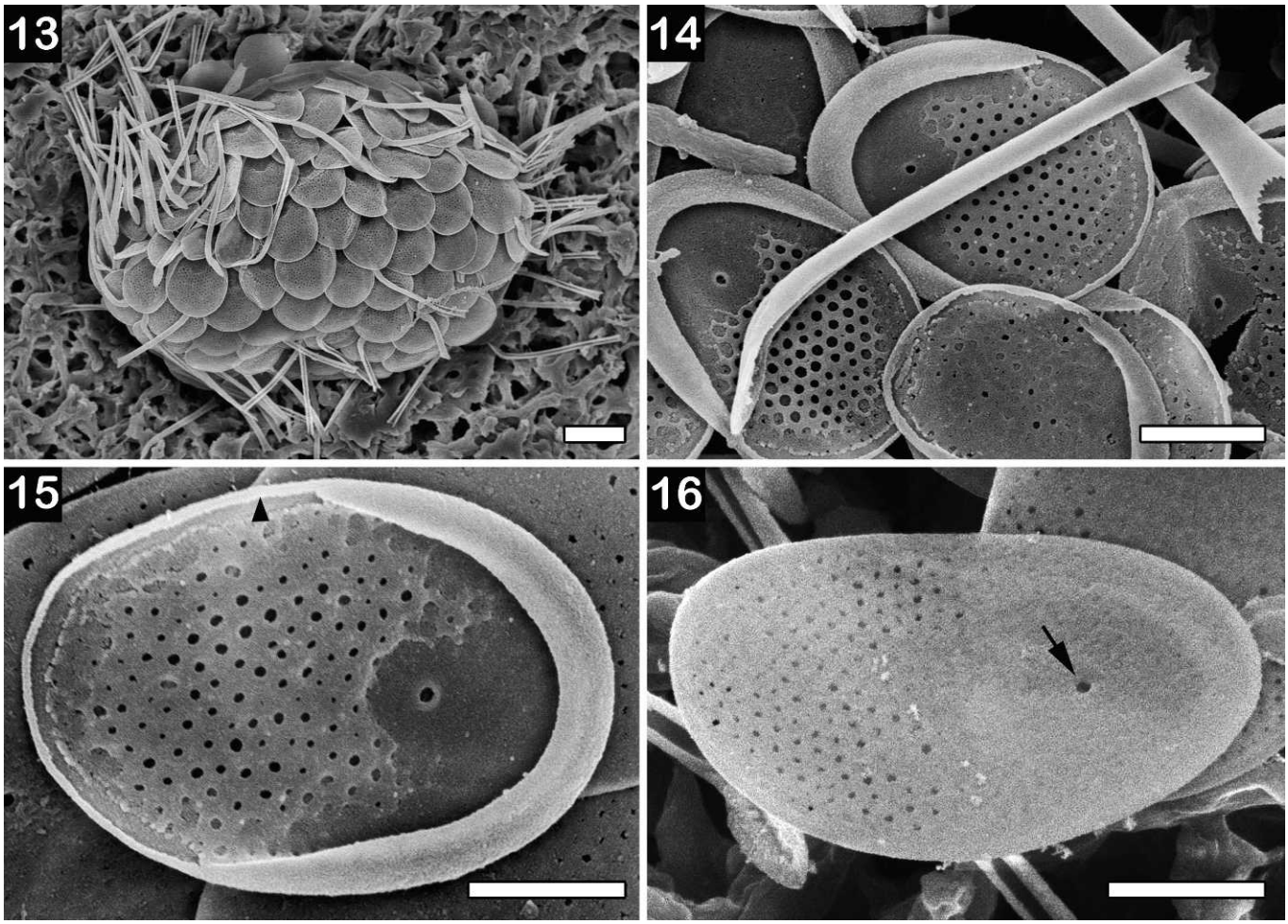

Figs 13–16. SEM micrographs of *Mallomonas pseudomatvienkoae* Gungnam052507A. For cells or scales, left sides on the figures are anterior, right sides are posterior. Scale bars = 1 μm.
Fig 13. Ellipsoid-shaped whole cell.
Fig 14. Bristle showing the proximal foot, a portion of the elongated slit, and an expanded, distal tip with teeth.
Fig 15. Top surface of a scale illustrating the thick secondary meshwork, single large pore, and posterior rim. Note that arrowhead is showing continuity of anterior rim with posterior upturned rim.
Fig 16. Bottom surface of the scale. Note that the base-plate pores are restricted to the anterior end of the scale.

AUTHENTIC CULTURE: CCMP 2880 deposited at the NCMA.

ETYMOLOGY: The Latin "lacuna" refers to the presence of scales with a pit.

Mallomonas hexareticulata Jo, Shin, Kim, Siver & Andersen *sp. nov.*

Figs 8–12

DESCRIPTION: Cells ellipsoidal (12–18 × 7–12 μm). Scales oval or obovoid, 2–5 × 2–3 μm; a posterior rim encircled half of the scale perimeter; irregular shaped base-plate pores restricted to the posterior one-third of the scale; distal two-thirds of the scale marked with a hexagonal secondary meshwork; a single large pore in the posterior scale region surrounded by a cluster of minute and smaller pores. Bristles 9–11 μm long, smooth, slightly curved and with a serrated distal tip; bristle shaft tubular, with a longitudinal slit.

HOLOTYPE: Collection of specimens on SEM stub deposited at the Herbarium of CNUK, Daejeon, Korea, CNU029285.

ISOTYPE: Collection of specimens on SEM stub deposited at the Herbarium of CNUK, Daejeon, Korea, CNU029700.

TYPE LOCALITY: Mudongji Pond, Muji-ri, Hwaseo-myeon, Mungyeong-si, Gyeongsangbuk-do, South Korea (36°26′43″N, 127°56′44″E), 24 July 2010.

ETYMOLOGY: The Latin specific epithet "*hexareticulata*" refers to the presence of scales with a hexagonal secondary meshwork.

Mallomonas pseudomatvienkoae Jo, Shin, Kim, Siver & Andersen *sp. nov.*

Figs 13–16

DESCRIPTION: Cells ellipsoidal (18–22 × 8–13 μm). Scales oval or obovoid, 3–5 × 2–3 μm; a posterior rim encircled about half of the

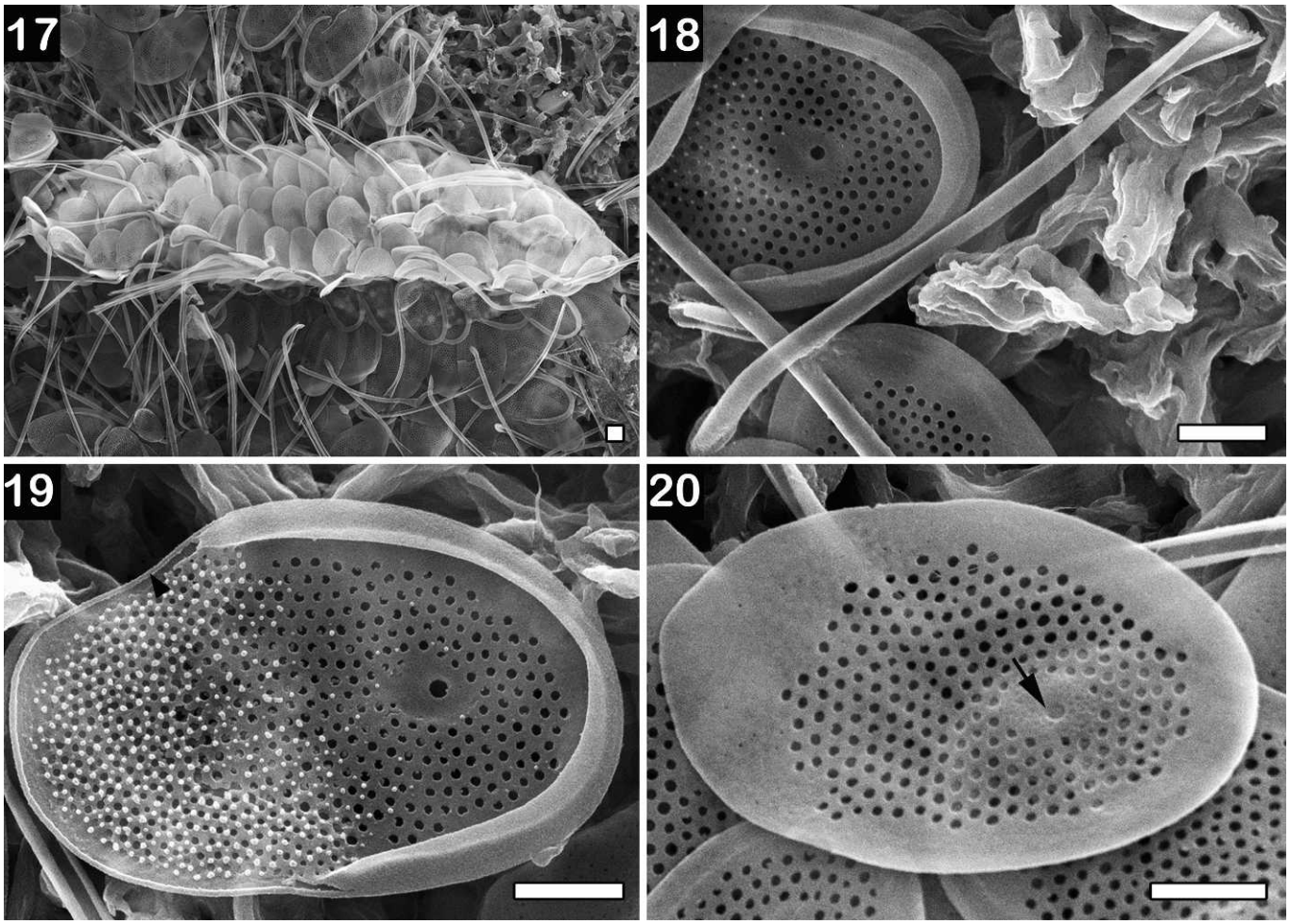

Figs 17–20. SEM micrographs of *Mallomonas sorohexareticulata* Gungnam092709. For cells or scales, left sides on the figures are anterior, right sides are posterior. Scale bars = 1 μm.
Fig. 17. Ellipsoid-shaped cell.
Fig. 18. Bristle showing the proximal foot, smooth side of the shaft, and an expanded distal tip with teeth.
Fig. 19. Top surface of a scale depicting small papillae, large-diameter base-plate pores, a single large pore within a hyaline zone, and the posterior rim. Note that arrowhead is showing continuity of the anterior rim with posterior upturned rim.
Fig. 20. Bottom surface of the scale illustrating the distribution of base-plate pores. Note the absence of pores near the posterior rim and along the anterior part of the scale.

perimeter of the scale; evenly spaced base-plate pores restricted to the distal half of the scale; posterior scale region with a large rimmed pore at the center; thick secondary meshwork covers the distal one-half to two-thirds of the scale. Bristles 5–9 μm long, smooth and slightly curved; bristle shaft with an open slit, and a bifurcated distal end bearing small teeth along one edge.

HOLOTYPE: Collection of specimens on SEM stub deposited at the Herbarium of CNUK, Daejeon, Korea, CNU029286.

ISOTYPE: Collection of specimens on SEM stub deposited at the Herbarium of CNUK, Daejeon, Korea, CNU029701.

TYPE LOCALITY: Gungnamji Pond, Buyeo-eup, Buyeo-gun, Chungcheongnam-do, South Korea (36°16′12″N, 126°54′46″E), 25 May 2007.

ETYMOLOGY: The specific epithet "*pseudomatvienkoae*" is derived from the species *M. matvienkoae* and Greek pseudo- (= false).

Mallomonas sorohexareticulata Jo, Shin, Kim, Siver & Andersen *sp. nov.*

Figs 17–20

DESCRIPTION: Cells ellipsoidal (28–36 × 7–15 μm). Scales oval or obovoid, 5–6.3 × 2–4 μm; a posterior rim encircled about one-half of the scale perimeter; large, evenly spaced base-plate pores; anterior scale region marked with small papillae; posterior scale region with a single large rimmed pore surrounded by a hyaline zone. Bristles 7–14 μm long, smooth, and slightly curved; bristle shaft with an open slit and an expanded distal end bearing a serrated margin.

HOLOTYPE: Collection of specimens on SEM stub deposited at the Herbarium of CNUK, Daejeon, Korea, CNU029287.

ISOTYPE: Collection of specimens on SEM stub deposited at the Herbarium of CNUK, Daejeon, Korea, CNU029702.

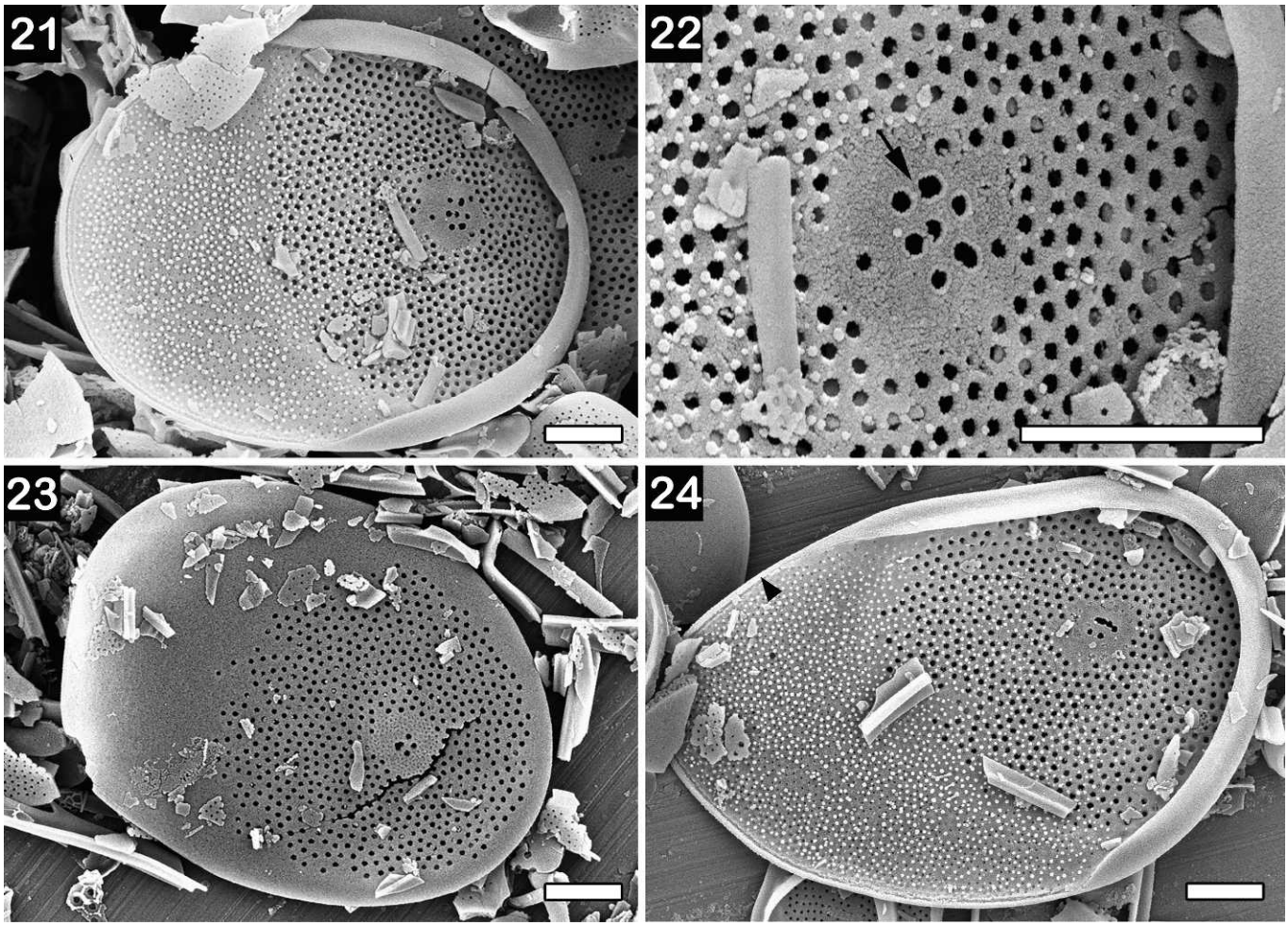

Figs 21–24. SEM micrographs of *Mallomonas pleuriforamen*. For cells or scales, left sides on the figures are anterior, right sides are posterior. Scale bars = 1 μm.

Fig. 21. Top view of fossil scales found in Eocene lake sediments from the Giraffe Pipe kimberlite. Note the distribution of surface papillae, the absence of base-plate pores on the anterior portion of the scale, and a series of four to seven large pores within a hyaline zone on the posterior end of the shield, and the posterior rim.

Fig. 22. Series of four to seven large pores within a hyaline zone on the posterior end of the shield, and the posterior rim.

Fig. 23. Bottom surface of the scale illustrating the distribution of base-plate pores. Note the absence of pores near the posterior rim and along the anterior part of the scale.

Fig. 24. Top view of fossil scales found in Eocene lake sediments from the Giraffe Pipe kimberlite. Note that arrowhead is showing continuity of the anterior rim with posterior upturned rim.

TYPE LOCALITY: Gungnamji Pond, Buyeo-eup, Buyeo-gun, Chungcheongnam-do, South Korea (36°16′12″N, 126°54′46″E), 27 September 2009.

ETYMOLOGY: The specific epithet "*sorohexareticulata*" is derived from the species *M. hexareticulata* and Latin *soro-* (= a sister of).

Mallomonas pleuriforamen Siver, Lott, Jo, Shin, Kim & Andersen *sp. nov.*

Figs 21–24

DESCRIPTION: Scales oval, large, from 6.8–7.4 × 5.6–6.3 μm in size. A posterior rim encircled half of the perimeter; evenly spaced base plate covered the proximal half to two-thirds of the scale; anterior half covered by small papillae; a cluster of four to seven large pores in posterior region surrounded by a hyaline zone.

HOLOTYPE: Collection of specimens on SEM stub deposited at the Canadian Museum of Nature, CANA 85745.

ICONOTYPES: Figs 21–24 (taken of the holotype).

TYPE MATERIAL: Slurry prepared from mudstone sample collected by PAS from section 13-1-80 of the Giraffe Pipe core and deposited at the Canadian Museum of Nature, CANA 85745.

TYPE LOCALITY AND SITE DESCRIPTION: Giraffe kimberlite, Northwest Territories, Canada (110°04′W, 64°48′N). The Giraffe locality contained well-preserved stratified organic sediment, including 68.3 m of lacustrine lake sediments overlain with 44.8 m of peaty material that constituted the posteruptive infilling of the maar crater that formed during emplacement of the kimberlite deposit (Siver & Wolfe 2005, 2009; Siver *et al.* 2009).

ETYMOLOGY: The specific epithet "*pleuriforamen*" is derived from Latin pleuri- (many) and Latin foramen (= pore) and refers to many large pores in the posterior region of the scale.

Table 2. Evolutionary models, log likehood values (–lnL), and model parameters indentified by the Modeltest 3.7 program (Posada and Crandall 1998) for individual and combined data sets (TrN + I + G).

Model parameter/data set	Nuclear LSU	Nuclear SSU	Plastid *rbc*L	Combined data set
−ln Likelihood	13,201.3975	6379.7715	3229.9451	23,500.5879
I	0.6354	0.6911	0.6845	0.6710
G	0.5947	0.6503	0.5963	0.6245
Base frequencies				
π_A	0.2959	0.2773	0.2974	0.2910
π_C	0.1938	0.1842	0.1835	0.1890
π_G	0.2600	0.2458	0.2743	0.2546
π_T	0.2503	0.2926	0.2448	0.2654
Rate matrix				
R_{AC}	1.0000	1.0000	1.0000	1.0000
R_{AG}	3.0364	3.8104	1.0235	2.7270
R_{AT}	1.0000	1.0000	1.0000	1.0000
R_{CG}	1.0000	1.0000	1.0000	1.0000
R_{CT}	6.6279	5.2675	2.2781	5.1380
R_{GT}	1.0000	1.0000	1.0000	1.0000
Aligned nucleotide	2576	1667	715	4958
Constant nucleotide	1957	1369	572	3898
MP-informative	450	222	107	779
MP-uninformative	169	76	36	281

This study contributed 67 new sequences; 23 sequences of nuclear-encoded SSU rDNA, 22 sequences of nuclear-encoded LSU rDNA, and 22 sequences of the plastid-encoded *rbc*L gene. For SSU rDNA, a fragment of about 1667 base pairs (bp) was obtained. For LSU rDNA, a fragment of about 2576 bp was obtained. For the plastid *rbc*L gene, a fragment of about 715 bp was obtained. A total of 3898 positions was constant, 1060 positions were variable, and 779 positions were parsimony-informative sites (Table 2). Among the 16 strains of *Mallomonas* representing section *Planae*, the similarity ranged from 94.4% to 100% and they had differences from 0 to 91 bp (Table S2).

The resulting phylogenetic tree strongly supported the existence of two major lineages, noted as C1 and C2 (Fig. 25). The C1 clade was comprised of members of the section *Planae* and the only species of the section *Heterospinae* used in the analysis. The C2 clade was much more diverse and comprised of members of the sections *Akrokomae*, *Annulatae*, *Insignes*, *Mallomonas*, *Papillosae*, *Planae*, *Punctiferae*, *Quadratae*, *Striatae*, and *Torqustae*. The C1 clade formed a monophyletic lineage (PP = 1.00 and ML, MP, and NJ BS = 100%) that included the new species. *Mallomonas peronoides* Momeu & Péterfi and *M. bangladeschica* (Takahashi & Hayakawa) Siver & Wolfe diverged at the base of the C1 clade, followed by *M. heterospina* Lund, *M. oviformis* Nygaard and by the taxa in the *M. matvienkoae* and *M. caudata* complexes (Fig. 25). The *M. oviformis* strains formed a sister group with *M. matvienkoae, M. psedomativienkoae, M. sorohexareticulata, M. hexareticulata, M. caudata,* and *M. lacuna*. *Mallomonas caudata* strains were closely related to *M. lacuna*, and *M. pseudomativienkoae* was most closely related to *M. matvienkoae*. The newly described species, *M. sorohexareticulata* and *M. hexareticulata*, were closely related to *M. matvienkoae* and *M. pseudomatvienkoae*.

The C2 clade formed a monophyletic lineage (PP = 1.00, ML = 73, and NJ BS = 100%), but not with the MP analysis. The C2 clade was further divided into two subclades. The first subclade, consisting of *M. insignis* Penard, *M. adamas* Harris & Bradley, *M. punctifera* Korshikov, *M. splendens* (West) Playfair, and *M. bronchartiana* Compère, was supported only by the Bayesian (PP = 1.00) and ML (BS = 85%) analyses. The *M. insignis* strains were strongly supported as a monophyletic group that diverged early within the C2 clade. The remaining four species were grouped together, but their relationships were not fully resolved. The second subclade, consisting of species with a V-rib and dome, also formed a monophyletic group. *Mallomonas mangofera* var. *forveata* (Dürrschmidt) Kristiansen of the section *Torquatae* diverged at the base of the second subclade, followed by the divergence of two additional groups. One group contained species from the sections *Mallomonas* and *Striatae* (PP =1.00, ML, MP and NJ BS = 100%), although taxa currently assigned to the section *Striatae* were not monophyletic. The remaining taxa, *M. akrokomos* (Ruttner) Pascher, *M. annulata*, and *M. papillosa* Harris & Bradley, formed a monophyletic lineage.

The origin of *Mallomonas* was estimated to be in the Early Jurassic (approximately 150 Ma), most likely between the Late Triassic and Early Cretaceous (205–105 Ma) (Fig. 26). Divergence of the C1 and C2 clades, representing species without and with a V-rib respectively, was estimated to have occurred during the Early Cretaceous at 133 Ma. Within C1

Fig. 25. Consensus Bayesian tree of the genus *Mallomonas* on the basis of a combination of nuclear SSU and LSU rDNA, and plastid *rbc*L sequence data. The Bayesian posterior probability (PP), maximum-likelihood (ML) bootstrap, maximum parsimony (MP), and distance values (NJ) are shown above or below the branches. The bold branches indicate strongly supported values (PP = 1.00 and ML, MP and NJ BS = 100%). Scale bar = 0.1 substitutions per site. →

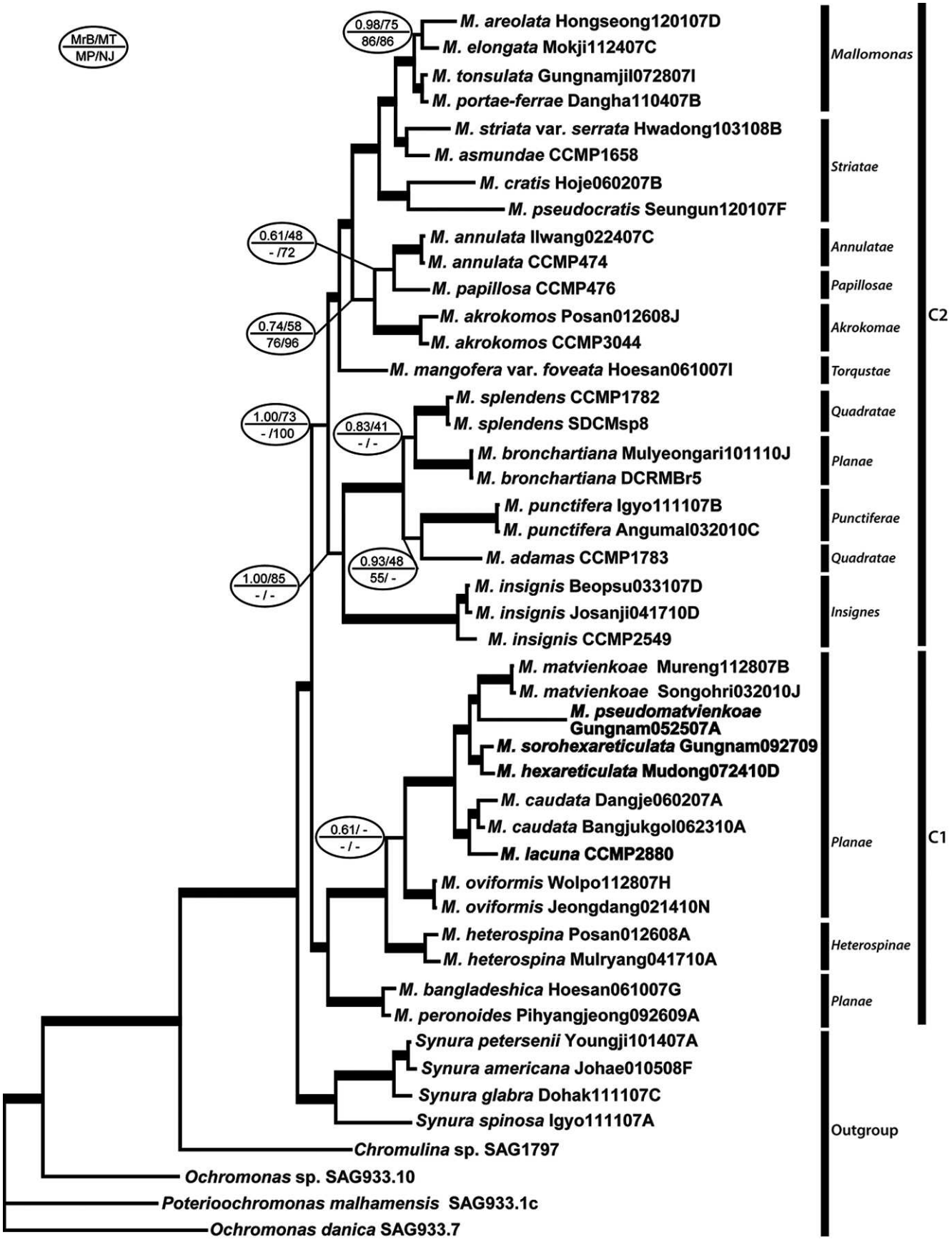
MrB/MT
MP/NJ
0.98/75
86/86
M. areolata Hongseong120107D
M. elongata Mokji112407C
M. tonsulata Gungnamjil072807I
M. portae-ferrae Dangha110407B
M. striata var. serrata Hwadong103108B
M. asmundae CCMP1658
M. cratis Hoje060207B
M. pseudocratis Seungun120107F
0.61/48
- /72
M. annulata Ilwang022407C
M. annulata CCMP474
M. papillosa CCMP476
0.74/58
76/96
M. akrokomos Posan012608J
M. akrokomos CCMP3044
M. mangofera var. foveata Hoesan061007I
1.00/73
- /100
0.83/41
- / -
M. splendens CCMP1782
M. splendens SDCMsp8
M. bronchartiana Mulyeongari101110J
M. bronchartiana DCRMBr5
M. punctifera Igyo111107B
M. punctifera Angumal032010C
0.93/48
55/ -
M. adamas CCMP1783
1.00/85
- / -
M. insignis Beopsu033107D
M. insignis Josanji041710D
M. insignis CCMP2549
M. matvienkoae Mureng112807B
M. matvienkoae Songohri032010J
M. pseudomatvienkoae Gungnam052507A
M. sorohexareticulata Gungnam092709
M. hexareticulata Mudong072410D
M. caudata Dangje060207A
M. caudata Bangjukgol062310A
0.61/ -
- / -
M. lacuna CCMP2880
M. oviformis Wolpo112807H
M. oviformis Jeongdang021410N
M. heterospina Posan012608A
M. heterospina Mulryang041710A
M. bangladeshica Hoesan061007G
M. peronoides Pihyangjeong092609A
Synura petersenii Youngji101407A
Synura americana Johae010508F
Synura glabra Dohak111107C
Synura spinosa Igyo111107A
Chromulina sp. SAG1797
Ochromonas sp. SAG933.10
Poterioochromonas malhamensis SAG933.1c
Ochromonas danica SAG933.7
Mallomonas
Striatae
Annulatae
Papillosae
Akrokomae
Torqustae
Quadratae
Planae
Punctiferae
Quadratae
Insignes
Planae
Heterospinae
Planae
Outgroup
C2
C1

clade, *M. peronoides* and *M. bangladeshica* diverged early at approximately 110 Ma. The subclade with *M. oviformis* and *M. heterospina* diverged from the subclade containing *M. caudata*, *M. matvienkoae*, and related taxa in the Late Cretaceous at about 73 Ma. Further proliferation within these two subclades occurred largely during the Paleogene.

The C2 clade diverged into two large subclades approximately 113 Ma during the Early Cretaceous (Fig. 26). *Mallomonas insignis* diverged from one of these subclades, and *M. mangofera* from the other, in the Late Cretaceous at around 96 Ma, and significant additional proliferation within both subclades took place largely during the Paleogene. Taxa that bear scales with large and well-developed domes, primarily found within the sections *Striatae* and *Mallomonas*, evolved in the Paleocene at approximately 61 Ma.

DISCUSSION

Morphologically, the scales of the five new species are characterized by a perforated basal plate with or without secondary structures, and the scales lack a V-rib. Five infraspecies of *M. matvienkoae* have been previously described (Kristiansen 2002) and were distinguished by the number of large pores found at the center of the distal region, the character of the reticulation, and the presence or absence of papillae. From a morphological point of view, except for *M. lacuna*, all of the newly described species bear some resemblance to *M. matvienkoae*, suggesting that these taxa are indeed closely related. However, clear and consistent differences in scale and bristle morphology unambiguously support the concept that the taxa represent different species. The differentiation of the new species is further supported by the molecular data. Of the newly described species, *M. pseudomatvienkoae* is most similar to the type for *M. matvienkoae* in terms of cell size, bristle morphology, and presence of secondary reticulation on the scale. However, this species differs from *M. matvienkoae* in that the base-plate pores are not distributed over the whole scale, but are restricted to the distal portion. The scale morphologies of *M. sorohexareticulata* and especially of the fossil taxon *M. pleuriforamen* are similar to *M. matvienkoae* var. *myakkana* Siver in that all three species have small papillae covering the distal portion of the scale. However, there are differences in the number of large pores found in the proximal portion of the scale and in the distribution of base-plate pores. Scales of *M. matvienkoae* var. *myakkana* have a cluster of three to five large proximal pores, whereas scales of *M. sorohexareticulata* have only one. Like *M. matvienkoae* var. *myakkana*, scales of *M. pleuriforamen* also have a cluster of pores, but there are often more than five pores and they are much smaller in diameter. In addition, the base-plate pores on *M. pleuriforamen* are distributed over a larger portion of the scale when compared with those on *M. matvienkoae* var. *myakkana*. Except for the large basket-like depression near the center of the scale, *M. lacuna* is virtually identical to *M. caudata*. In summary, ultrastructural differences of the siliceous components provide a useful means of separating not only sections, but also species within *Mallomonas*.

The phylogeny of *Mallomonas* species inferred in this study was consistent with the ones presented by Jo *et al.* (2011) and Siver *et al.* (2013), and those two papers also found that the genus had diverged into two major lineages. As suggested by Jo *et al.* (2011), the two clades can be distinguished on the basis of the morphology of the scales, in particular whether or not the scales have a V-rib. The C1 clade of our analyses consists of the *Planae* species, all of which lack a V-rib, whereas the C2 clade comprises the remaining species with a V-rib. However, phylogenetic relationships among species of the C2 clade were not fully resolved and this clade appears to further diverge into two major subclades. Additional taxon sampling and more genes should help to resolve the relationships within the C2 clade.

The separation of the four new modern species on the basis of scale and bristle structure is confirmed by the phylogenetic analysis. In the molecular analyses, three of the new species (*M. pseudomatvienkoae*, *M. sorohexareticulata*, *M. hexareticulata*) and *M. matvienkoae* are grouped together and form a sister clade to *M. caudata* and *M. lacuna*. The species within the series *Matvienkoae* of the section *Planae* have scales with secondary thickenings such as papillae or reticulation, whereas the latter two species within the series *Caudata* lack a secondary layer. However, relationships between *M. oviformis* (series *Matvienkoae*, section *Planae*) and *M. heterospina* (series *Heterospinae*, section *Heterospinae*) were not fully resolved. The scale of *M. oviformis* lacks a V-rib and dome and is covered with papillae. However, it also lacks the large proximal pore(s) and on the basis of this feature probably should be removed from the series *Matvienkoae*. *Mallomonas heterospina* also lacks a characteristic V-rib, but has a relatively small dome and a series of thick ribs on the shield. Therefore, the section *Planae* should be redefined to include *M. heterospina* as suggested by Jo *et al.* (2011), perhaps as a series.

On the basis of the Bayesian relaxed clock analysis, *Mallomonas* originated between the Late Permian (*c.* 258 Ma) and Late Jurassic (*c.* 137 Ma) and most likely in the Early Jurassic. This estimate is younger than the *c.* 331 Ma origin deduced from the chronogram of Boo *et al.* (2010). The difference is likely due to a much more comprehensive taxon sampling, coupled with a more comprehensive integration of the fossil record for *Mallomonas* (Siver & Wolfe 2005, 2009). Our estimates also suggest that divergence of the two main clades of *Mallomonas*, largely on the basis of the evolution of the V-rib structure, occurred close to the Late Jurassic–Early Cretaceous transition. Last, it is important to remember that our estimates represent minimum ages largely on the basis of fossil remains from the Giraffe Pipe locality. If older fossils are uncovered from other sites, the estimates will undoubtedly change.

ACKNOWLEDGEMENTS

This study was supported by the survey of Indigenous Biological Resources of Korea and Korean Tree of Life research program from National Institute of Biological Resources to WS; grants DEB-0716606, DEB-1049583 and DEB-1144098 to PAS from the US National Science

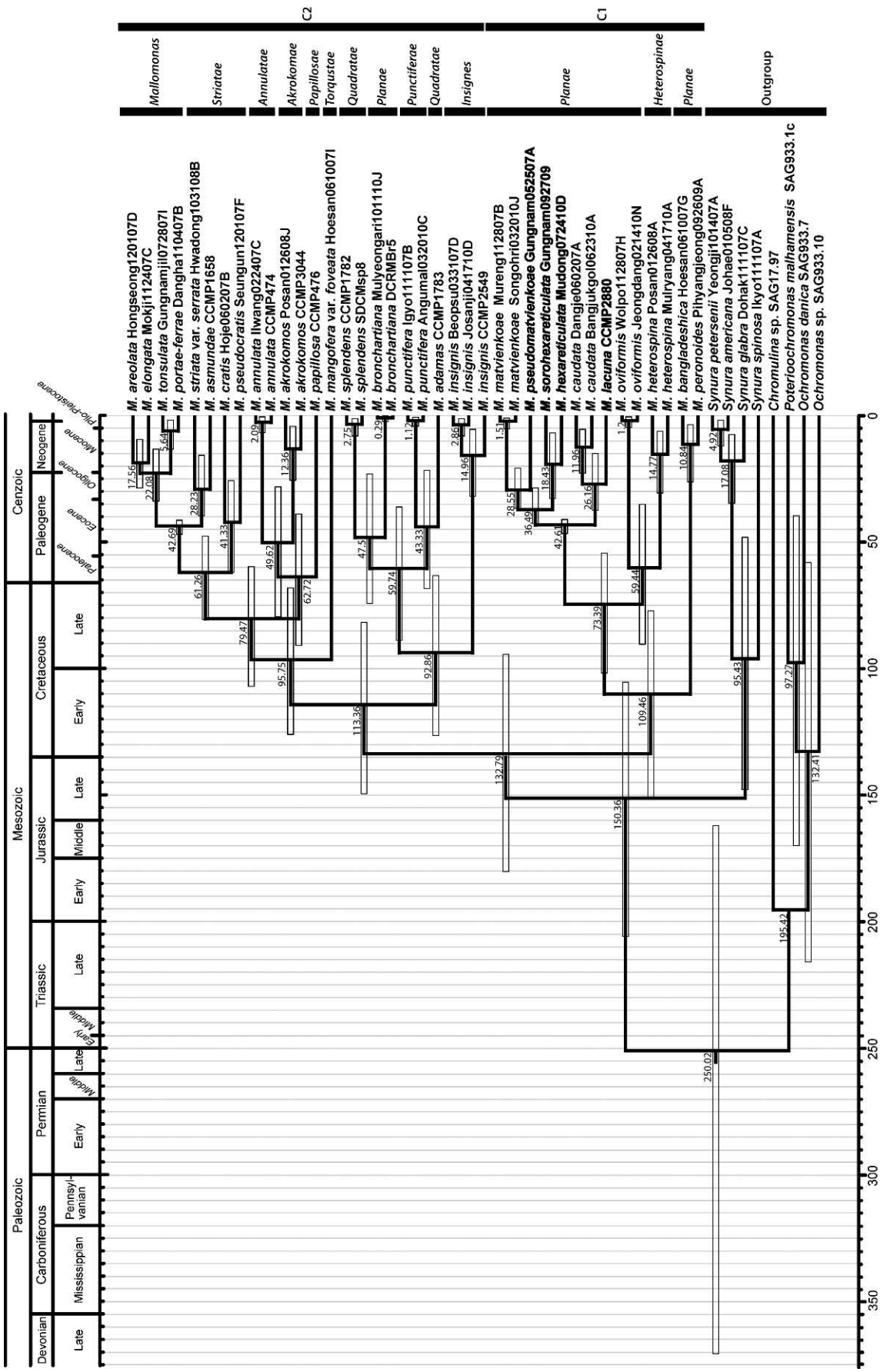

Fig. 26. A timescale of the genus *Mallomonas* from a Bayesian molecular clock analysis performed with BEAST.

Foundation; grant DEB 0949211 to RAA from the US National Science Foundation.

SUPPLEMENTARY DATA

Supplementary data associated with this article can be found online at http://dx.doi.org/10.2216/12–107.1.s1.

REFERENCES

Asmund B. & Kristiansen J. 1986. The genus *Mallomonas* (Chrysophyceae). A taxonomic survey based on the ultrastructure of silica scales and bristles. *Opera Botanica* 85: 1–128.

Belcher J. H. 1969. Some remarks upon *Mallomonas papillosa* Harris and Bradley and *M. calceolus* Bradley. *Nova Hedwigia* 18: 257–270.

Boo S. M., Kim H. S., Shin W., Boo G. H., Cho S. M., Jo B. Y., Kim J. H., Kim J. H., Yang E. C., Siver P. A., Wolfe A. P., Bhattacharya D., Andersen R. A. & Yoon H. S. 2010. Complex phylogeographic patterns in the freshwater alga *Synura* provide new insights into ubiquity vs. endemism in microbial eukaryotes. *Molecular Ecol*ogy 19: 4328–4338.

Conrad W. 1933. Revision du genre *Mallomonas* Perty (1852) incl. *Pseudo-Mallomonas* Chodat (1920). *Mémoires de Musée Royal d'Histoire Naturelle de Belgique* 56: 1–82.

Drummond A. J. & Rambaut A. 2007. BEAST: Bayesian evolutionary analysis by sampling trees. *BMC Evolutionary Biology* 7: 214–221.

Drummond A. J., Ho S. Y. W., Phillips M. J. & Rambaut A. 2006. Relaxed phylogenetics and dating with confidence. *PLoS Biology* 4: 699–710.

Harris K. & Bradley D. E. 1960. A taxonomic study of *Mallomonas*. *Journal of General Microbiology* 22: 750–77.

Ho S. & Phillips M. J. 2009. Accounting for calibration uncertainty in phylogenetic estimation of evolutionary divergence times. *Systematic Biology* 58: 367–380.

Huelsenbeck J. P. & Ronquist F. 2001. MRBAYES: Bayesian inference of phylogenetic trees. *Bioinformatics* 17: 754–755.

Jo B. Y., Shin W., Boo S. M., Kim H. S. & Siver P. A. 2011. Studies on ultrastructure and three-gene phylogeny of the genus *Mallomonas* (Synurophyceae). *Journal of Phycology* 47: 415–425.

Krieger W. 1930. Untersuchungen über Plankton-Chrysomonaden. *Botanisches Archiv* 29: 258–329.

Kristiansen J. 2002. The genus *Mallomonas* (Synurophyceae): a taxonomic survey based on the ultrastructure of silica scales and bristles. *Opera Botanica* 139: 1–218.

Kristiansen J. & Preisig H. R. 2007. Chrysophyte and haptophyte algae. Part 2: Synurophyceae. In: *Süßwasserflora von Mitteleuropa* (Ed. By B. Büdel, G. Gärtner, L. Krienitz, H.R. Preisig & M. Schagerl), 252 pp. Springer-Verlag, Berlin.

Matvienko A. M. 1941. Do systematiki rody *Mallomonas* (a contribution to the taxonomy of the genus *Mallomonas*). *Trudy Institutu Botaniky Kharkov* 4: 41–47.

Momeu L. & Péterfi L. S. 1979. Taxonomy of *Mallomonas* based on the fine structure of scales and bristles. *Contributions to Botany Cluj-Napoca* 19: 13–20.

Posada D. & Crandall K. A. 1998. MODELTEST: testing the model of DNA substitution. *Bioinformatics* 14: 817–818.

Siver P. A. 1991. The biology of *Mallomonas*: morphology, taxonomy, and ecology. Kluwer Academic Publishers, Dordrecht, the Netherlands. 228 pp.

Siver P. A. & Wolfe A. P. 2005. Eocene scaled chrysophytes with pronounced modern affinities. *International Journal of Plant Sciences* 166: 533–536.

Siver P. A. & Wolfe A. P. 2009. Tropical ochrophyte algae from the Eocene of Northern Canada: a biogeographic response to past global warming. *PALAIOS* 24: 129–135.

Siver P. A., Lott A. M. & Wolfe A. P. 2009. Taxonomic significance of asymmetrical helmet and lance bristles in the genus *Mallomonas* (Synurophyceae) and their discovery in Eocene lake sediments. *European Journal of Phycology* 44: 447–460.

Siver P. A., Wolfe A. P., Rohlf F. J., Shin W. & Jo B. Y. Combining morphological and molecular approaches to assess evolutionary patterns in *Mallomonas* (Synurophyceae: Heterokontophyta). *Geobiology* 2013 11: 127-138..

Stamatakis A. 2006. RAxML-VI-HPC: maximum likelihood-based phylogenetic analyses with thousands of taxa and mixed models. *Bioinformatics* 22: 2688–2690.

Swofford D. L. 2002. PAUP*: Phylogenetic analysis using parsimony (*and other methods). Version 4.0.b10. Sinauer Associates, Sunderland, Massachusetts.

Wuyts J., De Rijk P., Van De Peer Y., Winkelman T. & De Wachter R. 2001. The European large subunit ribosomal RNA database. *Nucleic Acid Research* 29: 175–177.

Received 6 September 2012; accepted 23 January 2013
Associate Editor: Ken-ichiro Ishida